

# STRESS ANALYSIS OF REINFORCED CONCRETE ANCHOR BLOCKS FOR UNDERGROUND PIPELINES USING FINITE ELEMENT METHOD

Dr. Nabeel A. Jasim and Dr. Adi Adnan Abdu-Alrazaq

University of Basrah-College of Engineering-Civil Engineering Department

## ABSTRACT

This paper deals with the behavior of reinforced concrete anchor blocks for underground steel pipelines under the effect of loads caused by internal pressure and temperature variation due to transportation of hydrocarbon products. The finite element method is used to carry out the analysis using ANSYS 5.4 program. To study the effect of soil, it is represented by springs with different values for modulus of subgrade reaction in normal and tangential reactions. It is concluded that increasing the values of the modulus of subgrade reactions,  $k_n$  and  $k_s$ , of the soil surrounding the reinforced concrete anchor block causes an increase in the failure loads of the block. But at high values of these modules, the rate of this increase in the failure load will decrease. The area of the passive face of the concrete anchor block is found to have the main effect on the failure load as compared to the length of that block. The failure load of the concrete anchor blocks that have square cross sections is 1.33 times larger compared to that of rectangular section. It is also concluded that locating the steel flange at middle of the block leads to larger resistance of anchor blocks as compared to any other position.

تحليل الاجهاد في الكتل المُثَبِّتة الخرسانية المسلحة في خطوط الانابيب المدفونة

باستخدام طريقة العناصر المحددة

د. عدي عدنان عبد الرزاق - د. نبيل عبد الرزاق حاسم

جامعة البصرة - كلية الهندسة - قسم الهندسة المدنية

## الخلاصة

يهدف البحث الحالي الى دراسة سلوك الكتل الخرسانية المسلحة والمستعملة لتثبيت الانابيب الفولاذية في خطوط نقل المنتجات النفطية تحت تأثير الضغط الداخلي والتغير في درجات الحرارة الناتج من نقل هذه المنتجات. استخدم برنامج ANSYS الهندسي لغرض احصاء التحليل بطريقة العناصر المحددة. تم تحليل الكتل المثبتة الخرسانية لغرض التحقق من تأثير أربعة عوامل تتضمن خصائص التربة الرمليّة، حجم وشكل الكتلة الخرسانية، موضع الحافة الفولاذية على طول الكتلة، موضع الانبوب ضمن الكتلة. ولغرض دراسة تأثير خصائص التربة على الكتلة الخرسانية، تم افتراض عدة قيم لمعامل رد فعل التربة بالاتجاهين العمودي والموازي للكتلة المثبتة. كذلك تم التحري عن تأثير احمال فعل التربة على بعض أوجه الكتلة الخرسانية. من خلال التحليل، تم التوصل الى أن زيادة قيم معاملات رد فعل التربة بالاتجاهين العمودي والموازي لأوجه الكتلة الخرسانية يؤدي الى زيادة الحمل الذي يحصل عنده الفشل، لكن معدل هذه الزيادة في حمل الفشل يقل مع ارتفاع قيم هذه المعاملات الى حدود عالية، ووجد أن مساحة مقطع الكتلة الخرسانية العمودي على اتجاه الانبوب لها التأثير الاكبر على حمل الفشل بالمقارنة مع طول الكتلة الموازي للانبوب. كما ان حمل الفشل للكتل الخرسانية ذات المقاطع المربعة يكون أكبر بمقدار 1.33 بالمقارنة مع الكتل ذات المقاطع المستطبة المتساوية لها بالحجم. كما ان أعلى مقاومة يمكن الحصول عليها للكتلة عندما ثبتت الحافة في منتصف الكتلة.

## Introduction

As pipelines, over or underground, are the means by which hydrocarbon products are conveyed between plant items, these pipelines are subjected to temperature variation, pressure and flow or combination of them that may cause movements in the pipeline.

In addition to the flexibility of the pipe system, there are several means by which, these movements can be controlled. For underground pipelines, concrete anchor blocks are often used to control these movements. Their function is to prevent translation and rotation of the pipe in any direction at the point of attachment [1].

Earliest study concerning with the stresses and deflections occurred in pipelines at the transition from fully restrained to unrestrained conditions was done by Schnackenberg [2]. Longitudinal deflections were used to determine whether a concrete anchor block is required, which separates the restrained portion from the moving portion of the line (Fig.1). The anchor force was expressed as [3,4]:

$$F_D = A_m [(0.5 - \nu) S_h + E\alpha(T_2 - T_1)] \dots\dots(1)$$

where  $A_m = \pi D t$  is the cross sectional area of the pipe in  $m^2$ ,  $D$ : mean diameter of the pipe,  $t$ : pipe wall thickness,  $S_h$ : hoop stress due to fluid pressure in  $kN/m^2$ ,  $\nu$ : Poisson's ratio,  $\alpha$ : thermal expansion coefficient in  $^{\circ}C^{-1}$ ,  $E$ : modulus of elasticity of steel pipe in  $kN/m^2$ ,  $T_1$ : temperature at time of installation in  $^{\circ}C$ ,  $T_2$ : maximum or minimum operating temperature in  $^{\circ}C$ .

The required bearing block area was given by [5]:

$$A_b = \frac{SF.F_D}{S_b} \dots\dots(2)$$

where,  $SF$ : is safety factor (usually 1.5),  $S_b$ : is the horizontal bearing strength of the soil;  $kN/m^2$ .

Peng [3,4] explained that special problems are involved in pipeline stress analysis because of the unique characteristics of a pipeline, code requirements, and techniques required in analysis. Elements of analysis were specified to include pipe movement, anchorage force, soil friction, lateral soil force, and soil-pipe interaction.

In the present study, the finite element method is used to analyze the stresses in the concrete anchor blocks. The different parameters that affect the design of such blocks are investigated.

### Modeling and Finite Element Formulation of the Materials

In this study, the reinforced concrete anchor block is analyzed by the finite element method (FEM), using the ANSYS 5.4 program. The model is made using

three-dimensional eight-noded brick elements, Solid65, as illustrated in Fig. (2) [6]. The element is defined by eight nodes having three degrees of freedom at each node (translations in x, y and z directions).

The concrete material is assumed to be non-linear isotropic and capable of directional integration point cracking and crushing. Cracking is permitted in three orthogonal directions at each integration point. If cracking occurs at an integration point, it is modeled through an adjustment of material properties which effectively treats the cracking as a smeared band of cracks.

The reinforcing steel is assumed to be smeared throughout the element and perfect bond between steel and concrete is assumed. The stress strain relationship for steel is assumed as bilinear with strain hardening.

The soil is assumed as sandy soil, with horizontal bearing capacity of  $192kN/m^2$ , which surrounding the anchor block at all sides except at the top. The soil is modeled using Combin14 spring element [6], which has also three degrees of freedom at each node. Each spring element is fixed at the far end to simulate infinite extended soil mass. Typical meshes used for simulation of the anchor block and surrounding soil are depicted in Fig. (3).

There are two types of Combin14 spring element, the first is normal to the faces of the anchor block to simulate the normal effect of the soil with coefficient of subgrade reaction ( $k_n$ ), while the other is tangential to the faces of the block to simulate the friction effect of the soil with coefficient of subgrade reaction ( $k_s$ ).

Full details can be found in Ref. [7].

### Analysis and Results

The full size models of anchor blocks, that have been analyzed, are designed according to the method of Refs. (2) and (3) in which the required failure load of the anchor blocks is computed from Eq. (1). In addition, some anchor blocks cast in the North Romaila site in Basrah, which were designed according to the same method, are

also reanalyzed. Figure (4) shows a typical concrete anchor block with its dimensions and reinforcement. The reinforcement ratio,  $\rho$ , is 0.0036.

According to the technical practice, a steel flange (ring of 10cm height and 5cm thickness) is welded to the pipe to prevent any slip between the pipe and the anchor block. Therefore, in this analysis the load is assumed to be transferred from the pipe to the concrete anchor block through this flange, whereas the material of the flange is neglected within the anchor block model. The load is assumed to distribute equally among the nodal points in front of the steel flange, as illustrated in Fig. (5). The load is applied at 30 equal increments.

The properties of the materials and the symbols used to designate them are shown in Table (1).

A detailed study is carried out to investigate the effect of the various parameters which are expected to control the design.

### 1: Effect of Soil Properties

To study the effect of changing the soil properties by changing the values of modulus of subgrade reaction, four different values of  $k_n$  and  $k_s$  were adopted using one model of anchor block, model 1, as given in Table (2A). The model has cross section dimensions designed according to the anchorage force given by Eq. (1), which is 886.5kN and exists in the site of North Romela in Basrah. The required area of model 1 was designed according to Eq. (2). The flange is placed at mid-length and mid-height of the blocks. The results of the analysis are given in Table (2B).

Table (2B) shows that the failure anchorage load increases as the values of  $k_n$  and  $k_s$  increase, but the rate of increasing of failure loads decreases with increasing of  $k_n$  and  $k_s$  values. This may be explained as that the increase of modulus of subgrade reaction will lead the soil to be more stiff and providing a confinement to the concrete material which improves its behavior. The model failed by crushing of concrete in

front of the flange for all values of  $k_n$  and  $k_s$ , as illustrated in Fig (6). The ratio of predicted failure load using finite element analysis to the design load ( $F_p/F_D$ ) ranges from 2.81 to 2.978 .

Figures (7) and (8) show, respectively, the stresses and strains along the block at the nodes located at the top of the pipe at the ultimate load. These figures show that the zone just behind the flange is under tension while the zone in front of the flange is under compression at failure.

As it can be seen maximum stresses occur at the zone in front of the flange where loads are applied. The maximum stresses are -22459kN/m<sup>2</sup>, -24145kN/m<sup>2</sup>, -23910kN/m<sup>2</sup>, and -24721kN/m<sup>2</sup> for  $k_n = 20000\text{kN/m}^3$ ,  $50000\text{kN/m}^3$ ,  $80000\text{kN/m}^3$ , and  $100000\text{kN/m}^3$ , respectively. While maximum strains are -0.0023, -0.00244, -0.00244, and -0.00244, respectively.

Figures (9) to (12) show the deformations of model 1 in different directions at different locations within the anchor block, remembering that there is symmetry about y-plane.  $U_z$  is the displacement in Z-direction,  $U_x$  in X-direction, and  $U_y$  in Y-direction. These figures show that increasing the values of subgrade reaction leads to a reduction in the deformations, but the rate of this reduction reduces with increasing the values of  $k_n$  and  $k_s$  due to the confinement provided by the stiff soil when  $k_n$  and  $k_s$  are increased.

Figures (9) and (10) show that Z-deformations of concrete close to the pipe at the zone in front of the flange have larger values compared to any other zone within the block. The deformations decrease with increasing the distance from the flange zone.

The same model 1 is also analyzed using constant values for modulus of subgrade reaction ( $k_n = 100000\text{kN/m}^3$ ,  $k_s = 12500\text{kN/m}^3$ ) under four cases as follows: (1) All springs on all faces are considered. (2) Neglecting the effect of the normal springs on the side faces by neglecting  $k_n$  on those faces. (3) Neglecting the effect of tangential spring on the side

faces and the base by neglecting  $k_s$  on them. (4) Neglecting the effect of the normal springs on the side faces and the tangential springs on the side faces and the base by neglecting  $k_n$  and  $k_s$ , respectively. The results of the analysis are given in Table (3).

Table (3) shows that the ratio of predicted failure load using finite element analysis to the design load ( $F_p/F_D$ ) ranges from 2.978 to 3.015. The model failed by crushing of concrete in front of the flange for all cases as explained in Fig. (6).

From the results, it is clear that neglecting the normal springs on the side faces, case 2, does not affect the failure load. Neglecting the tangential springs on the side faces and the base, case 3, causes the failure load to increase about (1.25%) greater than that of case 1. In case 4, where all normal springs on the side faces and tangential springs on the side faces and the base are neglected, the failure load is as for case 3.

The maximum stresses and strains occurred at the zone in front of the flange where loads are applied. Their values are  $-24721\text{kN/m}^2$ ,  $-23995\text{kN/m}^2$ ,  $-23927\text{kN/m}^2$ ,  $-24264\text{kN/m}^2$  and  $-0.00244$ ,  $-0.00244$ ,  $-0.00242$ ,  $-0.00244$  for cases 1, 2, 3, and 4, respectively.

## 2: Size of the Anchor Block

The required bearing area of the concrete anchor blocks can be found by Eq. (2), while there is no experimental or empirical technique to find the length of the anchor blocks, expect that the allowable bearing capacity of soil must not be exceeded. Therefore, the effect of size of the anchor block is studied by designing the bearing area according to the above equation, while the length will be varied using different values to find the length at which the block will resist the applied loads safely.

The model adopted in this study (model 2) is designed to withstand the anchorage force given by Eq. (1). Constant values for modulus of subgrade reactions are used ( $k_n = 100000\text{kN/m}^3$ ,  $k_s = 12500\text{kN/m}^3$ ). Model

2 has bearing area of ( $16\text{ m}^2$ ). To study the effect of the length of the concrete anchor blocks on their behavior, five different values of length were adopted, as listed in Table (4). The flange is assumed to be placed at the middle of the length and height of the concrete anchor blocks.

Table (4) shows that the ratio of predicted failure loads using finite element analysis to the design load ( $F_p/F_D$ ) ranges from 0.946 to 1.31. This Table shows that the failure load increases with increasing the length of the block, but the rate of load increase reduces for large values of length. This may be interpreted due to that failure always occurred in the zone in front of flange.

Figures (13) and (14) show the values of stresses and  $U_z$ -deformations in the Z-axis along the block, at top of the pipe. The maximum stresses, strains, and deformations occur at the zone in front of flange where crushing of concrete occurs at that zone.

The maximum stresses and strains for lengths 0.28m, 0.34m, 0.42m, 0.48m, and 0.56m are  $-22376\text{kN/m}^2$ ,  $-23910\text{kN/m}^2$ ,  $-24619\text{kN/m}^2$ ,  $-22879\text{kN/m}^2$ ,  $-20679\text{kN/m}^2$  and  $-0.00212$ ,  $-0.00228$ ,  $-0.00238$ ,  $-0.00224$ ,  $-0.00204$ , respectively.

The  $U_x$ -deformations along the Z-axis at the side faces and  $U_y$ -deformations along the Z-axis at the base increase with increasing the length of the blocks, as shown in Figs. (15) and (16).

$U_x$ -deformations increase from the active face toward the passive one except for lengths of 0.28m and 0.34m. While  $U_y$ -deformations change their values from positive (tension) at the active face of the block, behind the flange, to negative values (compression) at the passive face, in front the flange, where they begin to increase toward the passive face. Also the results for  $L= 0.28\text{m}$  and  $0.34\text{m}$  differ from those for other lengths.

## 3: Shape of the Concrete Anchor Block

The effect of the shape of cross sectional area of the passive face on the

behavior of the concrete anchor blocks is studied using two models of constant area and length, models 3 and 4. Model 3 has a square section, while model 4 has rectangular, as listed in Table (5). The modulus of subgrade reactions for the two models are ( $k_n = 100000\text{kN/m}^3$ , and  $k_s = 12500\text{kN/m}^3$ ). The flange is assumed to be placed at the middle of the length and height of the concrete anchor blocks.

Table (5) shows that the failure load for the anchor block of square section is 1.33 times greater than that of rectangular cross section. In the two models, the concrete anchor blocks failed by crushing of concrete in front of the flange.

Figure (17) shows that stresses along Z-axis, at top of the pipe, behind the flange are close together for the blocks of the two models, while in front of flange, model 3 have stresses greater than that of model 4.

Maximum stress for the model 3 is  $-22534\text{kN/m}^2$  and for model 4 is  $-21332\text{kN/m}^2$ . While, the maximum strain for the model 3 is  $-0.0022$  and for model 5 is  $-0.00202$ .

Figure (18) shows the  $U_x$ -deformations along the side faces. The determined  $U_x$  for model 3 is larger as compared to that of model 4. This behavior is due to the larger distance of side faces from the pipe zone for model 4 compared to that of model 3, as mentioned previously. Due to same reason, the  $U_y$ -deformations along the Z-axis for the base of block at model 4 are larger as compared to that of model 3 as shown in Fig. (19).

#### 4: Position of the Flange along the Concrete Anchor Block

The effect of position of the pipe flange on the behavior of concrete anchor block is studied through that the flange was assumed to be placed at different seven positions along pipe of model 1, as listed in Table (6). Constant values for modulus of subgrade reactions are assumed ( $k_n = 100000\text{kN/m}^3$ , and  $k_s = 12500\text{kN/m}^3$ ). The properties of the reinforced concrete anchor block and surrounding soil are listed in Table (1).

Table (6) shows that the maximum failure load occurred at the case when the flange is located at face of anchor block ( $3102.0\text{kN}$ ), when  $z = 0.0\text{m}$ . Within the anchor block, the maximum failure load occurred in the case when flange is located at the mid-length of the block ( $2640.0\text{kN}$ ), when  $z = 1.25\text{m}$ . In all cases, the concrete anchor blocks failed by crushing of concrete in front of the flange. The failure load when the flange is located at the active face is greater by 17.5% as compared to that when it is at the mid-length of the block.

Making a comparison between the predicted failure loads using finite element analysis and the design failure load,  $F_F/F_D$ , this ratio ranges from 2.08 to 3.5.

Figure (20) shows the failure load variation with the position of pipe flange. The load is larger when the flange is within first half of the block. The maximum value is obtained at the mid-length of the block, and then it decreases with increasing distance toward the passive face of the block. The largest value of failure load is obtained when the flange is placed at the active face, but this is not preferable practically since it is structurally advantageous to contain the flanged zone of pipe within the concrete block, in addition to that the concrete block provides a protection to the flange from aggressive attack of soil.

Thus, it can be noted that the best position for the flange to insure larger resistance capacity is at the mid-length of the block.

#### 5: Position of the Pipe within the Anchor Block

In some cases, the pipe may not located in the mid-height of the concrete anchor blocks, but it may be placed at the bottom third of the block. To study the effect of this parameter and comparing this with the case at which the pipe is located at mid-height of the anchor blocks, a model is examined using the two cases. In the first case, the pipe is located at the mid-height of the anchor block, model 1. In the second

case, the pipe is placed at distance 0.5m from the base, model 5. Two positions of the flange are selected for each case. The first is at the active face of the block,  $z = 0.0\text{m}$ , while the second is at the mid-length of the block,  $z = 1.25\text{m}$  from the active face, as listed in Table (7). This table shows that failure loads of model 1 are greater than that of model 5 by average value of 9% for both  $z = 0$  and  $z = -1.25\text{m}$ .

In the two models, the concrete anchor blocks failed by crushing of concrete in front of flange where maximum stresses, strains and deformations occurred.

For model 1, the maximum stresses are  $-24721\text{kN/m}^2$  and  $-24277\text{kN/m}^2$  for  $z = 0$  and  $z = -1.25\text{m}$ , respectively, while the maximum strains are  $-0.00252$  and  $-0.00244$ , respectively. These values are larger than those of model 5, in which the maximum stresses and strains for  $z = 0$  and  $z = -1.25\text{m}$  are  $-24001\text{kN/m}^2$ ,  $-22478\text{kN/m}^2$  and  $-0.00236$ ,  $-0.00222$ , respectively.

The  $U_y$ -deformations in model 5 have larger values as compared to those of model 1 (Fig. 21). This is because the distance from the pipe to the base for model 5 is smaller and remembering that deformations gradually decrease with increasing distance from the pipe or the flange zone. For the two cases of flange's position in model 1,  $U_y$ -deformations changed their values from positive at the active face to negative with increasing distance towards the passive face, while this behavior is reversed in model 5.

### Conclusions

Based on the finite element stress analysis of the reinforced concrete anchor blocks, the following main conclusions can be drawn:

- 1- The failure of concrete anchor blocks occurs by crushing of concrete at the zone in the front of flanges, where the larger values of stresses and strains have occurred.
- 2- Increasing the values of the modulus of subgrade reactions of the soil surrounding the reinforced concrete anchor block,  $k_n$  and  $k_s$ , causes an increasing in the failure

loads. But the increase in failure load occurs at decreasing rate as the  $k_n$  and  $k_s$  values become larger.

- 3- Increasing the values of the moduli of subgrade reactions,  $k_n$  and  $k_s$ , causes a decrease in the values of deformations.
- 4- The increase in the length of the anchor block increases the failure load of the block, but it seems that a length more than 0.4m have no influence, provided that the soil bearing capacity is not violated.
- 5- The area of the passive face of the concrete anchor block has the main effect on the failure load.
- 6- The load capacities of the concrete anchor blocks that have square sections are 1.33 times larger than that of rectangular section.
- 7- The load capacity of the concrete anchor block when the pipe is placed at mid-height of the block is 9% larger than that when the pipe is placed at the bottom third of the block.
- 8- To insure the adequate load capacity for the block and best fixity between the pipe material and the concrete anchor block, the best position for the flange is at the center of the block.

### References

- 1- "Handbook of Industrial Pipework Engineering", McGraw-Hill Book Company (UK) Limited, 1973.
- 2- Schnackenberg, P. J.; "How to Calculate Stress in above/below Ground Transition", Pipe Line Industry, November, 1976, pp. 53-56.
- 3- Liang-Chuan Peng; "Stress Analysis Methods for Underground Pipelines", Part 1, Pipe Line Industry, April, 1978, pp. 67-72.
- 4- Liang-Chuan Peng; "Stress Analysis Methods for Underground Pipelines". Part 2, Pipe Line Industry, May, 1978, pp. 65-74.
- 5- "Thrust Restraint Design for Ductile Iron Pipe", DIPRA, Ductile Iron Pipe Research Association, 1997.

- 6- ANSYS; "Element Reference", Release 5.4, Swanson Analysis Systems, Inc., 1997.  
7- Abdu-Alrazaq, Adi Adnan; "Stress

Analysis of Reinforced Concrete Anchor Blocks for Underground Pipelines Using Finite Element Method", Ph. D. Thesis, University of Basrah, 2007.

**Table (1): Properties of the Concrete and Steel Reinforcement for the Modeled Anchor Block and Surrounding Soil.**

Material	Parameter	Symbol	Value
Concrete of the anchor block	Unit weight (kN/m <sup>3</sup> )	$\gamma_c$	23.1
	Young's Modulus (kN/m <sup>2</sup> )	$E_c$	$21.2 \times 10^6$
	Ultimate uniaxial cylinder compressive strength	$f'_c$	20000
	Ultimate uniaxial tensile strength (kN/m <sup>2</sup> )	$f_t$	1800
	Poisson's ratio	$\nu_c$	0.2
Steel reinforcement	Unit weight (kN/m <sup>3</sup> )	$\gamma_s$	78.9
	Young's Modulus (kN/m <sup>2</sup> )	$E_s$	$2 \times 10^8$
	Poisson's ratio	$\nu_s$	0.3
Soil	Unit weight (kN/m <sup>3</sup> )	$\gamma_{soil}$	22
	Angle of internal friction	$\phi$	35°
Steel of the* pipe	Young's Modulus (kN/m <sup>2</sup> )	$E_p$	$2 \times 10^8$
	Poisson's ratio	$\nu_p$	0.3
	Thermal expansion coefficient (°C <sup>-1</sup> )	$\alpha$	$10.8 \times 10^{-6}$

\* For design requirement.

**Table (2A): Details of Model 1.**

Model No.	Pipe dia. (D <sub>o</sub> ) (m)	Dimensions of the modeled block (m)				No. of Element	No. of loaded Nodes	Modulus of subgrade reaction (kN/m <sup>3</sup> )		
		Height (H)		Width (W)				k <sub>n</sub>	k <sub>s</sub>	
1	0.1524*	1.5		3.0		2.5	3696	88	20000	2500
									50000	6250
		80000	10000							
		100000	12500							
		$h_1$	$h_2$	$w_1$	$w_2$					
		0.75	0.75	1.5	1.5					

\*Pipe thickness = 11mm.

**Table (2B): Predicted Failure Loads for Model 1.**

Model No.	Design factored load (F <sub>D</sub> )* (kN)	Modulus of subgrade reaction (kN/m <sup>3</sup> )		Failure Load using FEM (F <sub>F</sub> ) (kN)	F <sub>F</sub> /F <sub>D</sub>
		k <sub>n</sub>	k <sub>s</sub>		
1	886.5	20000	2500	2491.5	2.810
		50000	6250	2565.0	2.893
		80000	10000	2600.4	2.933
		100000	12500	2640.0	2.978

\* Schnackenberg<sup>(2)</sup> method.

Table (3): Predicted Failure Loads for Model 1.

Model No.	Design factored load ( $F_D$ )* (kN)	Case	Failure Load using FEM ( $F_F$ ) (kN)	$F_F/F_D$
1	886.5	1	2640.0	2.978
		2	2644.0	2.983
		3	2673.0	3.015
		4	2673.0	3.015

\* Schnackenberg<sup>(2)</sup> method.

Table (4): Dimensions and Predicted Failure Loads for Model 2.

Model No.	Pipe Dia. ( $D_p$ ) (m)	Design factored load ( $F_D$ )* (kN)	Designed area ( $m^2$ )	Dimensions of ** concrete anchor blocks (m)			H/L	No. of Eleme.	No. of Loaded Nodes	Failure Load ( $F_F$ ) (kN)	$F_F/F_D$
				Height (H)	Width (W)	Length (L)					
2	0.508	3000.0	16.00	4.00	4.00	0.28	14.29	7200	240	2826.0	0.94
						0.34	11.76			3240.0	1.08
						0.42	9.52			3852.0	1.28
						0.48	8.33			3870.0	1.29
						0.56	7.14			3916.5	1.31

\* Schnackenberg<sup>(2)</sup> method.\*\*  $h_1 = h_2 = w_1 = w_2 = 2.00$  m, Pipe thickness = 8.7mm.

Table (5): Dimensions and Predicted Failure Loads for Models 3 and 4.

Model No.	Pipe Dia. ( $D_p$ ) (m)	Designed factored load ( $F_D$ )* (kN)	Designed area ( $m^2$ )	Dimensions of concrete anchor blocks (m)				No. of Eleme.	No. of Loaded Nodes	Failure Load ( $F_F$ ) (kN)	$F_F/F_D$	
				Height (H)		Width (W)						Length (L)
3	0.406**	1733.4	9.00	3.00		3.00		0.48	4608	192	3096.0	1.79
				$h_1$	$h_2$	$w_1$	$w_2$					
				1.5	1.5	1.50	1.50					
4	0.406**	1733.4	9.00	2.00		4.50		0.48	4576	208	2324.4	1.34
				$h_1$	$h_2$	$w_1$	$w_2$					
				1.0	1.0	2.25	2.25					

\* Schnackenberg<sup>(2)</sup> method.

\*\* Pipe thickness = 6.4mm.

Table (6): Predicted Failure Loads for Model 1.

Model No.	Design factored load ( $F_D$ )* (kN)	Position of flange from active face (m)	Failure Load ( $F_F$ ) (kN)	$F_F/F_D$
1	886.5	0.00	3102.0	3.50
		0.357	2409.0	2.72
		0.714	2508.0	2.83
		1.25	2640.0	2.98
		1.607	2620.0	2.96
		1.964	1873.5	2.11
		2.32	1848.0	2.08

\* Schnackenberg<sup>(2)</sup> method.



Table (7): Predicted Failure Loads for Models 1 and 5.

Model No.	Design factored load ( $F_D$ )* (kN)	No. of Elements	No. of Loaded Nodes	Position of flange from active face (m)	Failure Load ( $F_F$ ) (kN)	$F_F/F_D$
1	886.5	3696	88	0.00	3102.0	3.50
				1.25	2640.0	2.98
5		3528	84	0.00	2835	3.20
				1.25	2430	2.74

\* Schnackenberg<sup>(2)</sup> method.

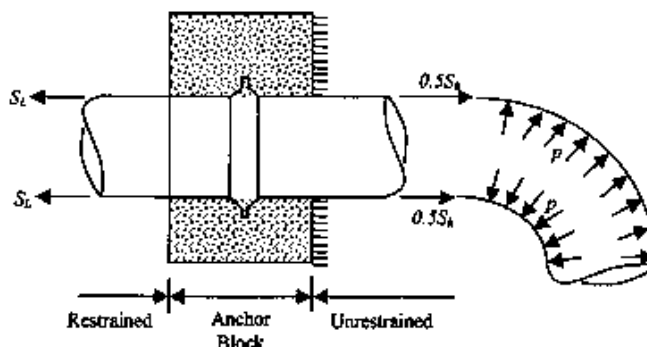


Fig. (1): Anchor Force, from Anchor Installed to Limit Movement of Pipe. [3]

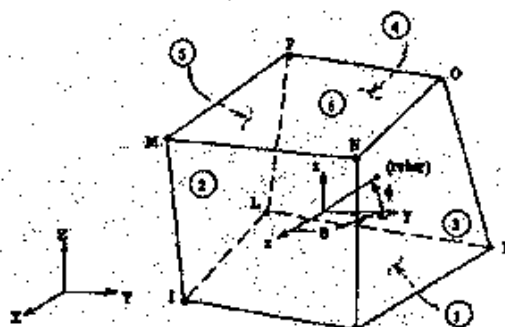


Fig. (2): Solid65 3-D Reinforced Concrete Element.

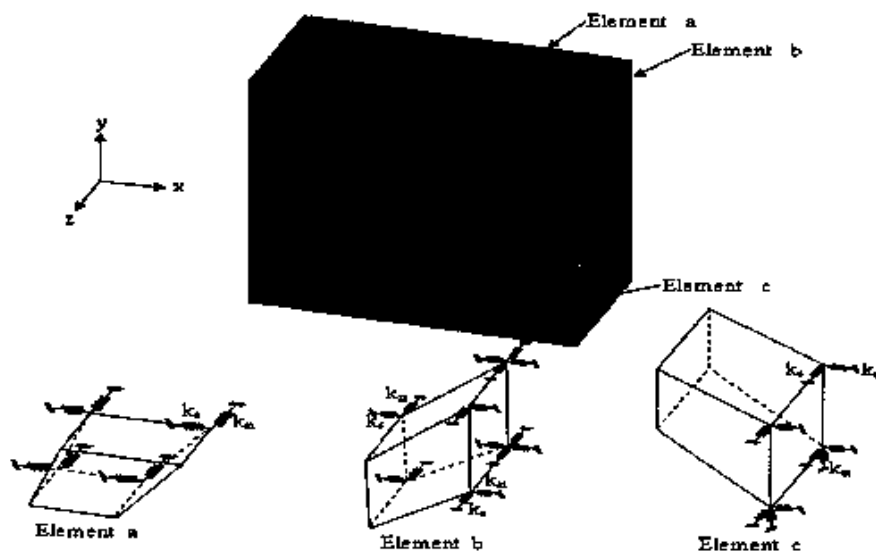


Fig. (3): Typical Meshes Used For Simulation of the Anchor Block and Surrounding Soil.

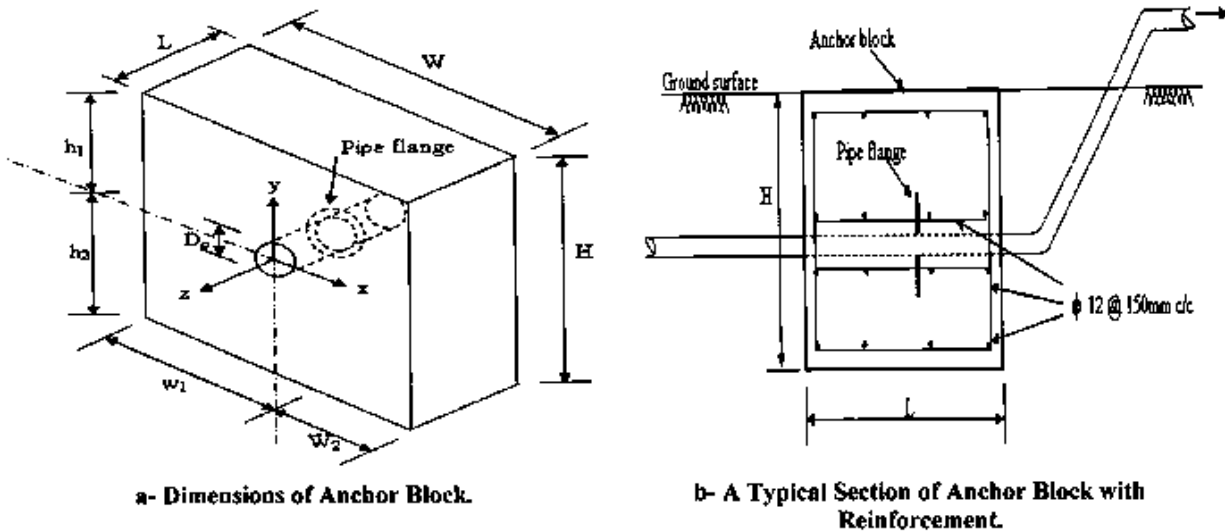


Fig. (4): Concrete Anchor Block.

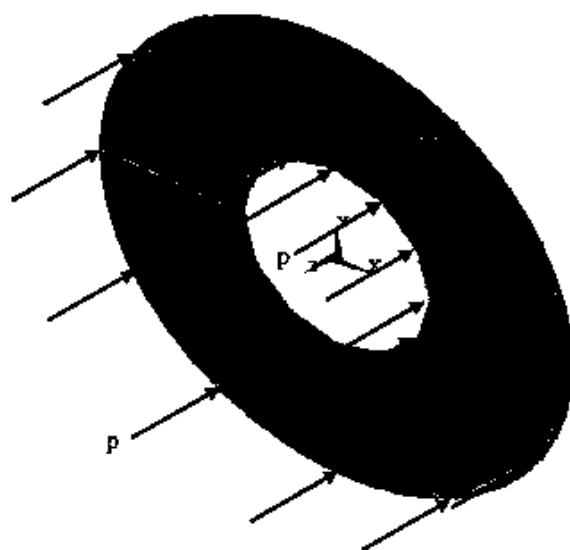


Fig. (5): Load Simulation.

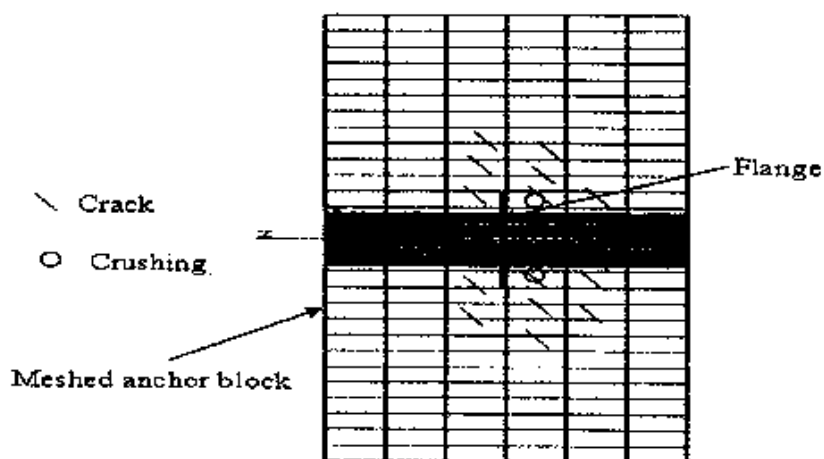


Fig. (6): Typical Cracks and Crushing.

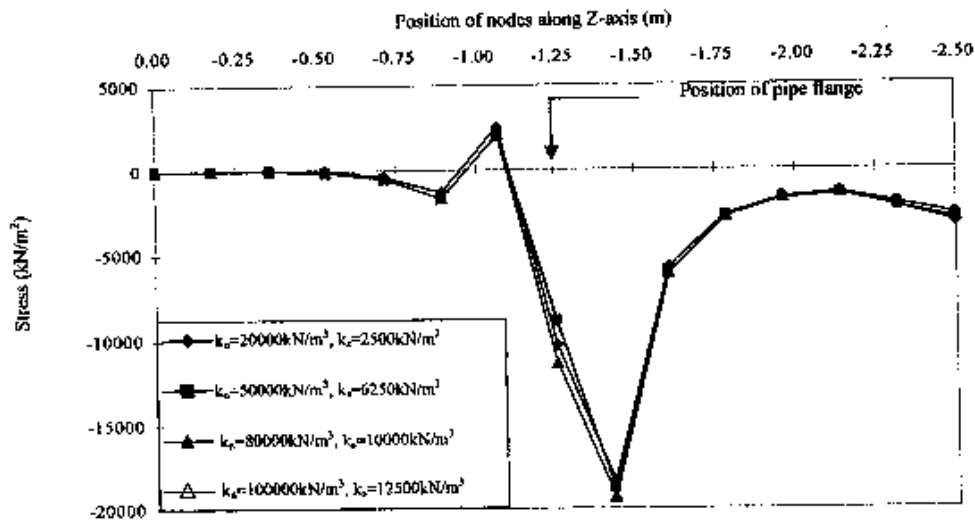


Fig: (7) Stresses-Position of Nodes along the Z-Axis for Model 1, at Top of Pipe.

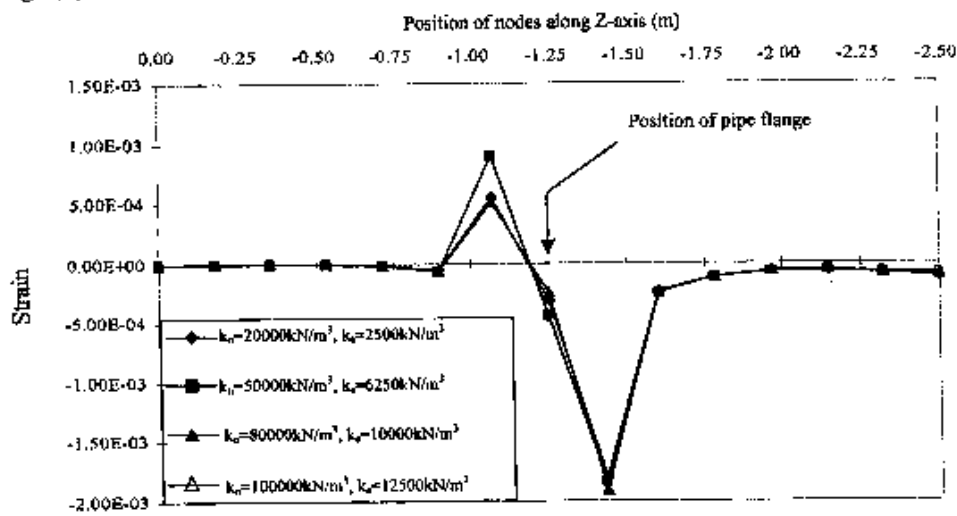


Fig: (8): Strains-Position of Nodes along the Z-Axis for Model 1, at Top of Pipe.

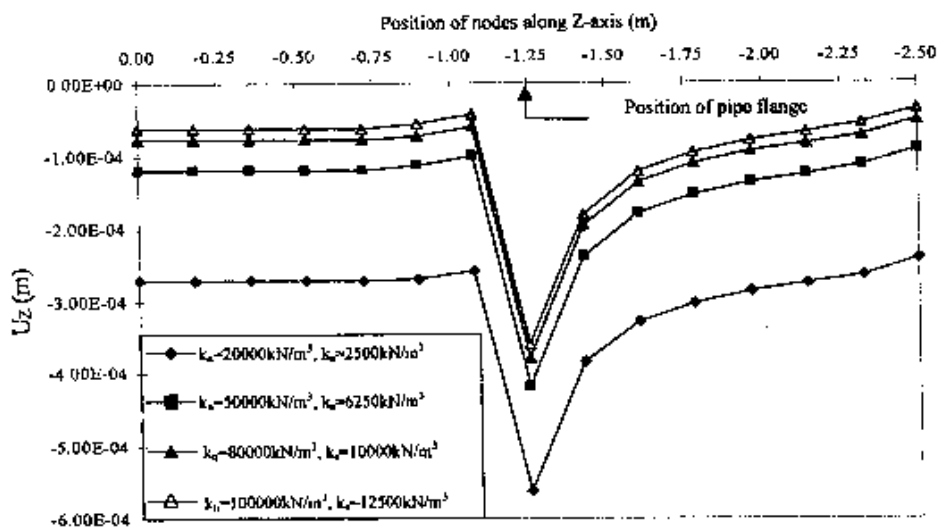


Fig. (9):  $U_z$ -Deformations of Nodes along Z-Axis at Top of Pipe.

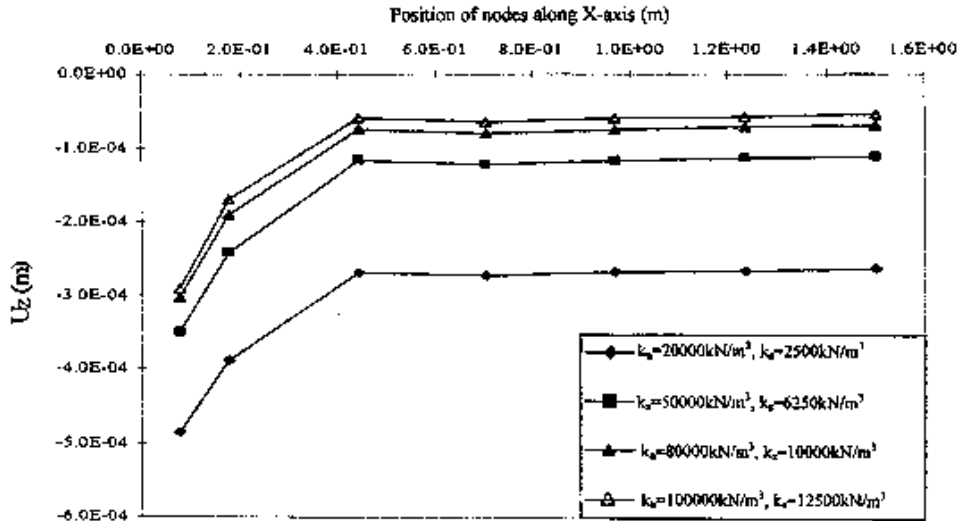


Fig. (10):  $U_z$ -Deformations of Nodes along X-Axis at Plane of Loading Flange.

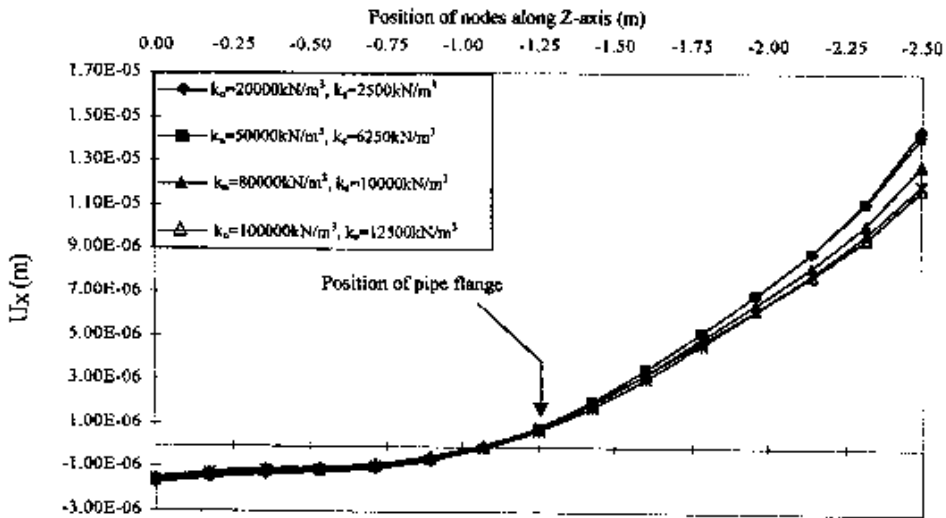


Fig. (11):  $U_x$ -Deformations of Nodes along Z-Axis at Middle of the Right Face.

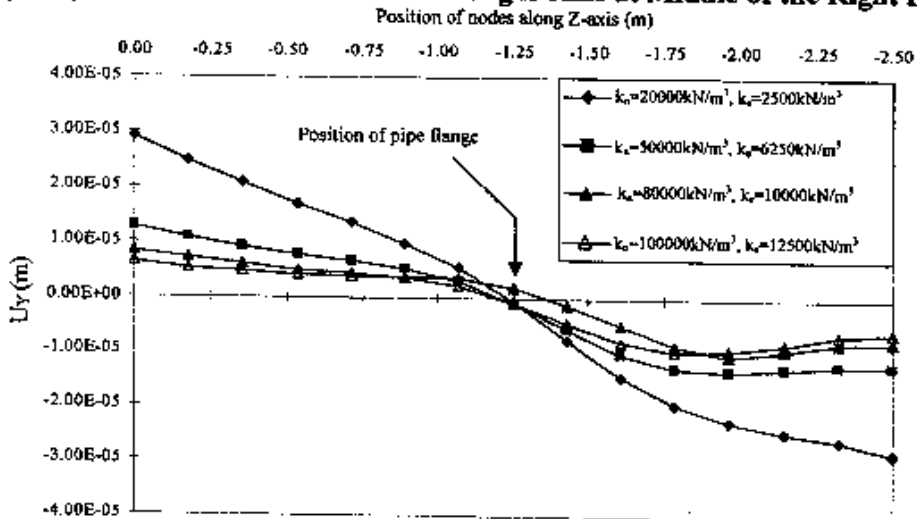


Fig. (12):  $U_y$ -Deformations of Nodes along Z-Axis at Middle of the Base.

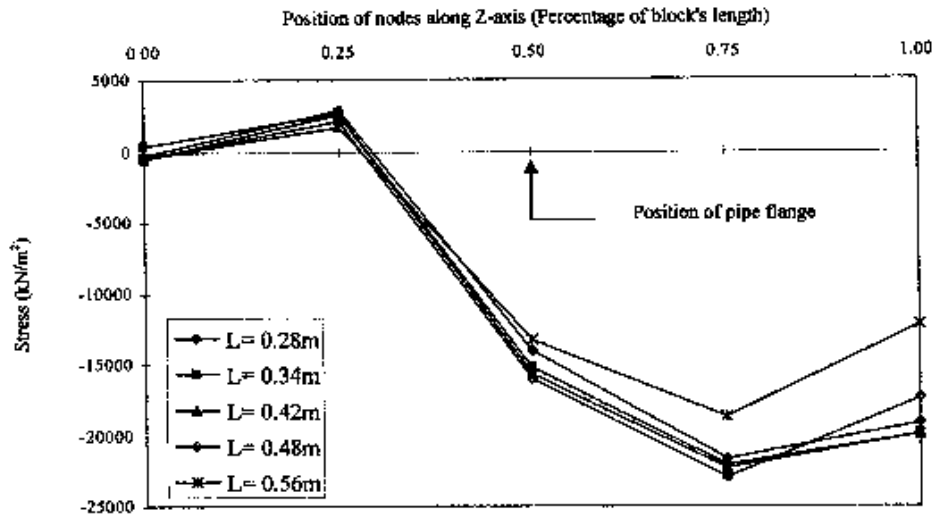


Fig. (13): Stresses-Position of Nodes along the Z-Axis for Model 2, at Top of Pipe.

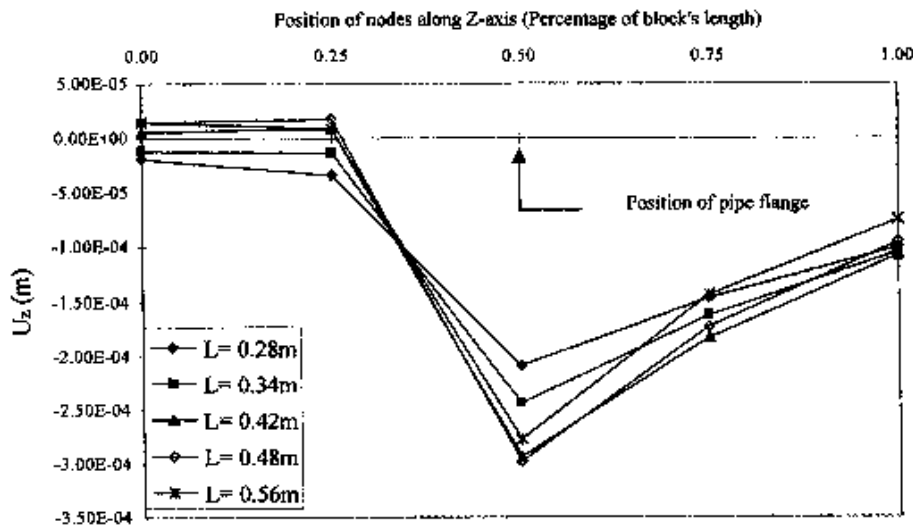


Fig. (14):  $U_z$ -Deformations of Nodes along Z-Axis for Model 2, at Top of Pipe.

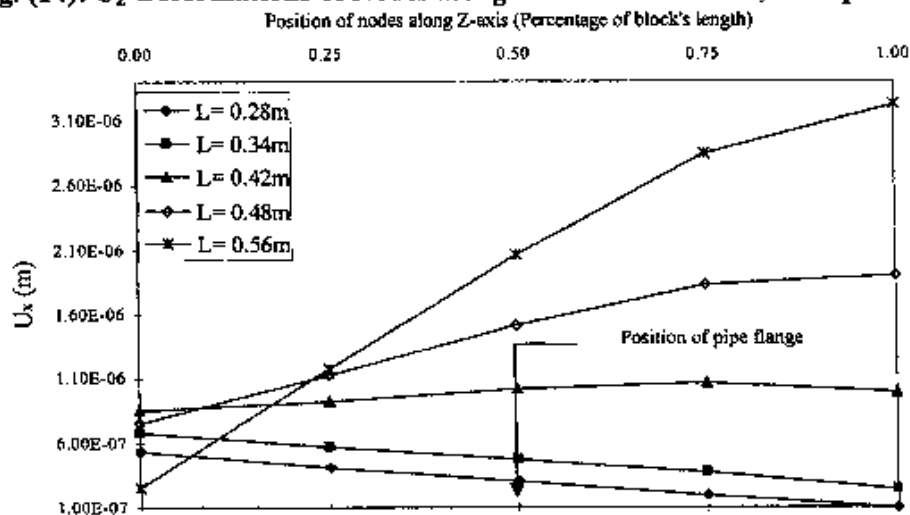


Fig. (15):  $U_x$ -Deformations of Nodes along Z-Axis for Model 2, at Middle of Right Face.

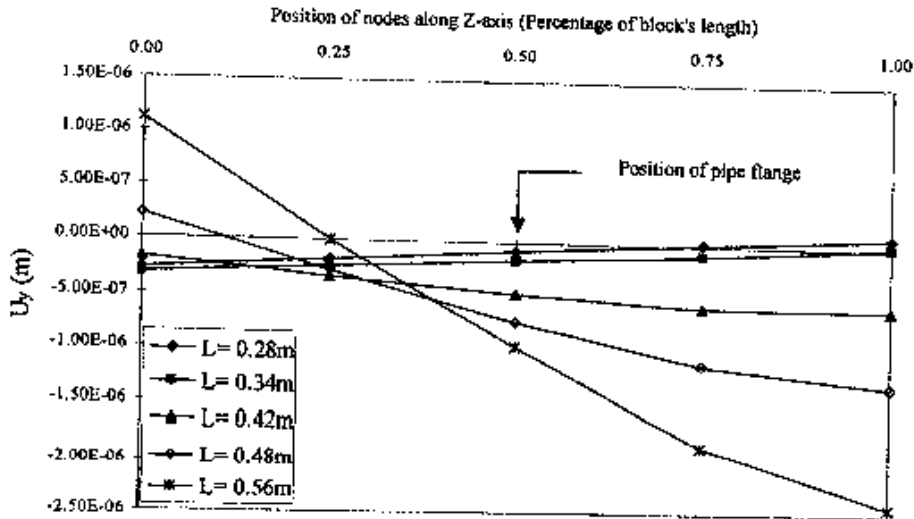


Fig. (16):  $U_y$ -Deformations of Nodes along Z-Axis for Model 2, at Middle of Base.

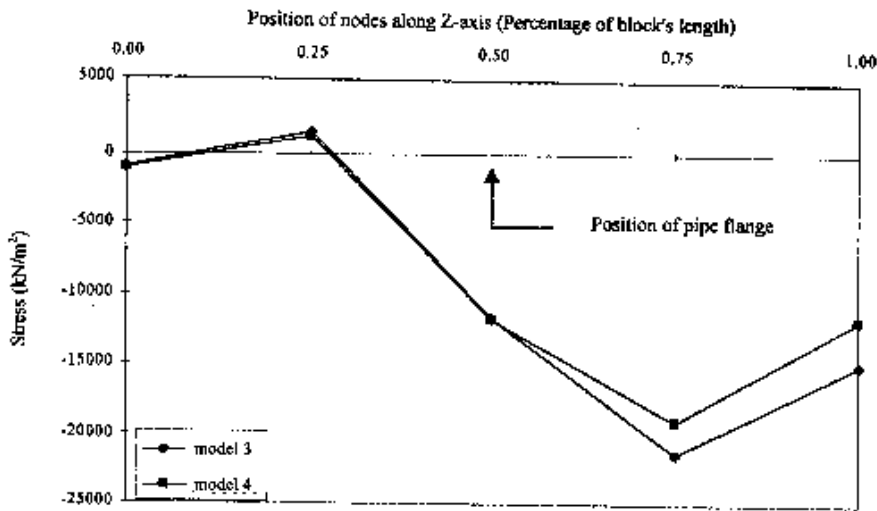


Fig. (17): Stresses-Position of Nodes along the Z-Axis for Models 3 and 4, at Top of Pipe.

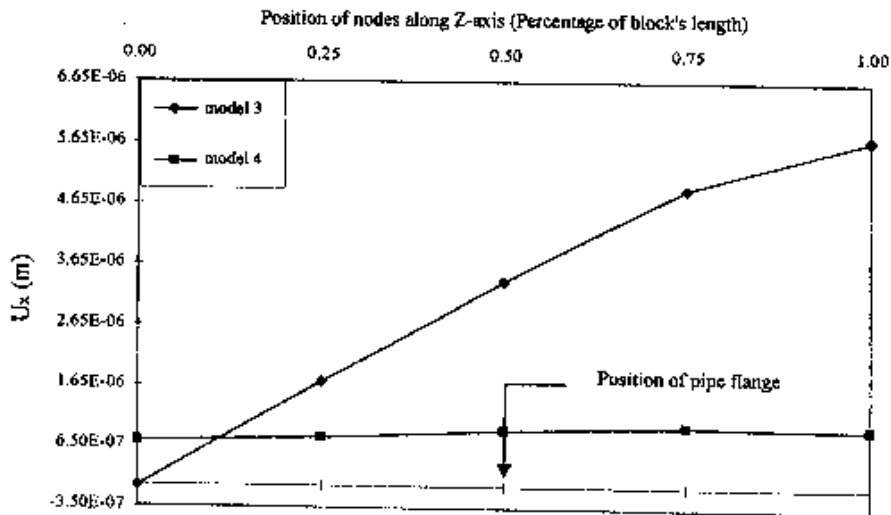


Fig. (18):  $U_x$ -Deformations of Nodes along Z-Axis for Models 3 and 4, at Middle of Right Face.

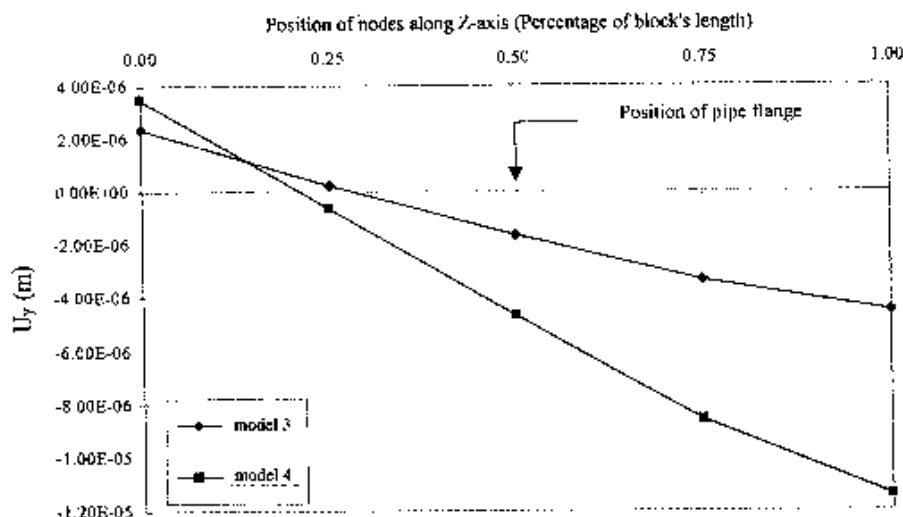


Fig. (19):  $U_y$ -Deformations of Nodes along Z-Axis for Models 3 and 4, at Middle of Base.

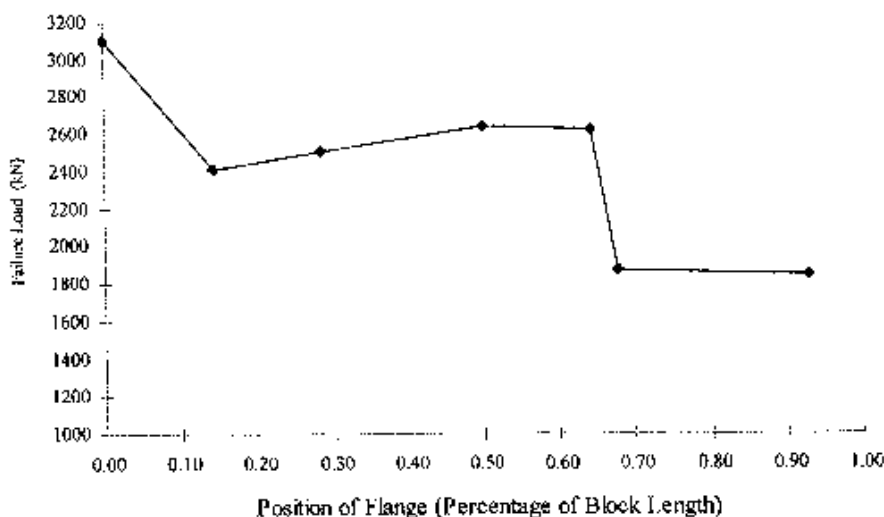


Fig. (20): Failure Load-Position of the Flange Relationship for Model 1

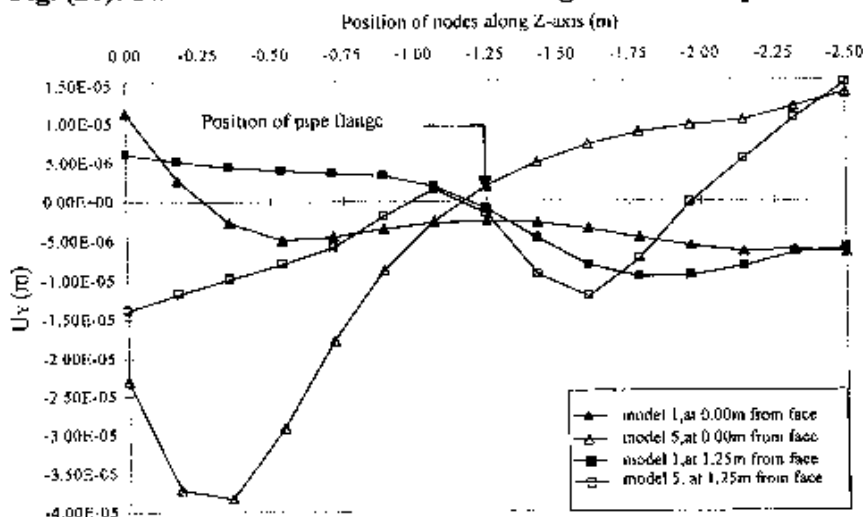


Fig. (21):  $U_y$ -Deformations of Nodes along Z-Axis for Models 1 and 5, at Middle of Base.